数理解析研究所講究録 1244 巻 2002 年 82-90

Multifractal Analysis of Turbulence by Statistics based on Non-Extensive Tsallis' or Extensive Rényi's Entropy

横国大・環情　　有光直子 (N. Arimitsu)
Graduate School of EIS, Yokohama Nat'l. University, Yokohama 240-8501, Japan

筑波大・物理　　有光敏彦 (T. Arimitsu)
Institute of Physics, University of Tsukuba, Ibaraki 305-8571, Japan

(October 31, 2001)

An analytical expression of probability density function (PDF) of velocity fluctuation is derived with the help of the statistics based on generalized entropy (the Tsallis entropy or the Rényi entropy). It is revealed that the derived PDF explains the detailed structure of experimentally observed PDF as well as the scaling exponents of velocity structure function. Every parameters appeared in the analysis, including the index proper to the Tsallis entropy or the Rényi entropy, are determined, self-consistently, by making use of observed value of intermittency exponent. The experiments conducted by Lewis and Swinney (1999) are analyzed.

47.27.-i, 47.53.+n, 47.52.+j, 05.90.+m

An investigation of turbulence based on the generalized entropy, Tsallis' [1,2] or Rényi's [3], was started by the present authors [4] with an investigation of the p-model [5,6] in terms of a generalized statistics constructed on the entropy. We intend to analyze the velocity fluctuation, $\delta u(r) = |u(x+r) - u(x)|$, between two points with a distance r apart in a turbulence. Here, u represents one of the components of the fluid velocity field $\vec{u}$, say x-component. By making use of the velocity fluctuation δu_0 of eddies with the largest size ℓ_0, the Reynolds number is estimated, in the absence of intermittency [7], as $\mathrm{Re} = \delta u_0 \ell_0 / \nu = (\ell_0/\eta)^{4/3}$ where ν and $\eta = (\nu^3/\epsilon)^{1/4}$ are, respectively, the kinematic viscosity and the Kolmogorov scale. The quantity ϵ represents the energy input rate at the largest eddies.

In the case of high Reynolds number $\mathrm{Re} \gg 1$, there exist a lot of steps, $n = 1, 2, \cdots$, at each of which eddies break up into two parts producing a energy cascade. The size of eddies in the nth step of the cascade is assumed to be given by $\ell_n = \delta_n \ell_0$ with $\delta_n = 2^{-n}$. Then, our main interest in the following reduces to the fluctuation of velocity difference $\delta u_n = \delta u(\ell_n)$ corresponding to the size of nth eddies in the cascade. Note that the dependence of the number of steps n_{K} on r/η, within the analysis where intermittency is not taken into account [7], is given by

$$n = -\log_2 r/\eta + (3/4)\log_2 \mathrm{Re}. \tag{1}$$

In this paper, we examine the experimental results obtained by Lewis and Swinney [16] for turbulent Couette-Taylor flow produced in a concentric cylinder system. Our analysis is based on the fact that, for high Reynolds number Re $\gg 1$, the Navier-Stokes equation for incompressible fluid is invariant under the scale transformation [6]: $\vec{r} \to \lambda^{\alpha/3}\vec{u}$, $\vec{u} \to \lambda\vec{r}$, $t \to \lambda^{1-\alpha/3}t$ and $(p/\rho) \to \lambda^{2\alpha/3}(p/\rho)$. Here, the exponent α is an arbitrary real quantity which specifies the degrees of singularity in the velocity gradient $|\partial u(x)/\partial x| = \lim_{\ell_n\to 0}|u(x+\ell_n)-u(x)|/\ell_n = \lim_{\ell_n\to 0}\delta u_n/\ell_n$. This can be seen with the relation $\delta u_n/\delta u_0 = (\ell_n/\ell_0)^{\alpha/3}$, which leads to the singularity in the velocity gradient [8] for $\alpha < 3$, since $\delta u_n/\ell_n^{\alpha/3} = \text{const.}$.

The distribution $P^{(n)}(\alpha)d\alpha \propto P^{(1)}(\alpha)^n d\alpha$ of singularities at the nth step in the cascade with

$$P^{(1)}(\alpha) \propto \left[1-(\alpha-\alpha_0)^2/(\varDelta\alpha)^2\right]^{1/(1-q)}, \tag{2}$$

$(\varDelta\alpha)^2 = 2X/[(1-q)\ln 2]$ was derived [9–12] by taking an extreme of the Tsallis entropy [1,2,13] $S_q^{\mathrm{T}}[P^{(1)}(\alpha)] = (1-q)^{-1}\left(\int d\alpha P^{(1)}(\alpha)^q - 1\right)$ which is non-extensive, or the Rényi entropy [3] $S_q^{\mathrm{R}}[P^{(1)}(\alpha)] = (1-q)^{-1}\ln\int d\alpha P^{(1)}(\alpha)^q$ which has the extensive character, with appropriate constraints, i.e., the normalization of distribution function, $\int d\alpha P^{(1)}(\alpha) = \text{const.}$, and the q-variance being kept constant as a known quantity, $\sigma_q^2 = \langle(\alpha-\alpha_0)^2\rangle_q = (\int d\alpha P^{(1)}(\alpha)^q(\alpha-\alpha_0)^2)/\int d\alpha P^{(1)}(\alpha)^q$. In deriving $P^{(n)}(\alpha)$, we assumed that each step in the cascade is statistically independent. Note that the values of α are restricted within the range $[\alpha_{\min}, \alpha_{\max}]$, where $\alpha_{\max}-\alpha_0 = \alpha_0-\alpha_{\min} = \Delta\alpha$.

With the help of the relation $P^{(n)}(\alpha) \propto \delta_n^{1-f(\alpha)}$ [6], we can extract the multi-fractal spectrum $f(\alpha)$ in the form [9–12]:

$$f(\alpha) = 1 + (1-q)^{-1}\log_2\left[1-(\alpha-\alpha_0)^2/(\Delta\alpha)^2\right], \tag{3}$$

which reveals how dense each singularity, labeled by α, fills physical space.

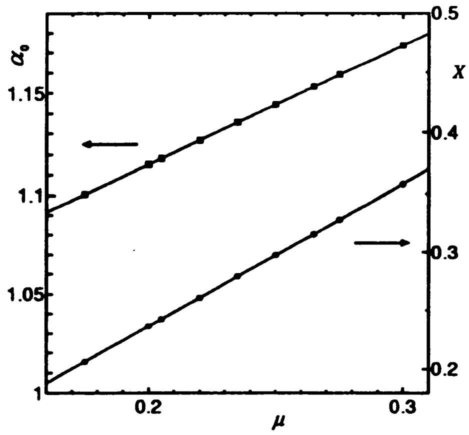

FIG. 1. The μ-dependence of α_0 and X. Squares and circles are the points where the self-consistent equations are solved.

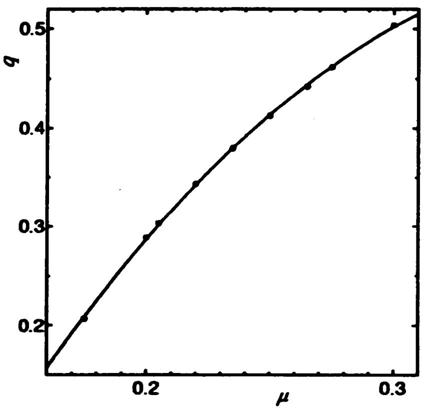

FIG. 2. The μ-dependence of q. Circles are the points where the self-consistent equations are solved.

By making use of an observed value of the intermittency exponent μ as an input, the quantities α_0, X and the index q can be determined, self-consistently, with the help of the three independent equations, i.e., the energy conservation: $\langle \epsilon_n \rangle = \epsilon$, the definition of the intermittency exponent μ: $\langle \epsilon_n^2 \rangle = \epsilon^2 \delta_n^{-\mu}$, and the scaling relation [9–12]: $1/(1-q) = 1/\alpha_- - 1/\alpha_+$ with $\alpha_\pm$ satisfying $f(\alpha_\pm) = 0$, where the average $\langle \cdots \rangle$ is taken by $P^{(n)}(\alpha)$. The scaling relation is a generalization of the one derived first by [14,15] to the case where the multi-fractal spectrum has negative values. The μ-dependences of the self-consistent solutions, α_0, X and q, are given in Fig. 1 and Fig. 2 for the region where the value of μ is usually observed, i.e., $0.16 \leq \mu \leq 0.31$. We see that they are given in this region by the equations $\alpha_0 = 0.998 + 0.587\mu$, $X = -5.73 \times 10^{-3} + 1.21\mu$ and $q = -0.607 + 6.01\mu - 7.72\mu^2$.

Adopting the value $\mu = 0.28$ observed in the experiment [16] with the Taylor-scale

Reynolds number $R_\lambda = 262$ (Re = 540 000) or $R_\lambda = 80$ (Re = 69 000), and solving the above three equations self-consistently, we have $q = 0.471$, $\alpha_0 = 1.162$, $X = 0.334$. Then, we obtain $\alpha_+ - \alpha_0 = \alpha_0 - \alpha_- = 0.748$, $\Delta\alpha = 1.350$ [9–12].

It may be reasonable to assume that the probability $\Pi^{(n)}(x_n)dx_n$ to find the scaled velocity fluctuation $|x_n| = \delta u_n/\delta u_0$ in the range $x_n \sim x_n + dx_n$ can be divided into two parts:

$$\Pi^{(n)}(x_n)dx_n = \Pi_{\rm N}^{(n)}(x_n)dx_n + \Pi_{\rm S}^{(n)}(|x_n|)dx_n \tag{4}$$

where the singular part $\Pi_{\rm S}^{(n)}(|x_n|)$, stemmed from multifractal distribution of singularities in velocity gradient that may be related to the fluctuations caused by turbulent viscosity, is determined by $\Pi_{\rm S}^{(n)}(|x_n|)dx_n = P^{(n)}(\alpha)d\alpha$ with the transformation of the variables between $|x_n|$ and α: $|x_n| = \delta_n^{\alpha/3}$, leading to [12]

$$\Pi_{\rm S}^{(n)}(|x_n|)dx_n = 3G^{(n)}(|x_n|)/\left(Z^{(n)}|\ln\delta_n|\right)dx_n \tag{5}$$

with

$$G^{(n)}(x) = x^{-1}\left[1 - (\alpha(x) - \alpha_0)^2/(\Delta\alpha)^2\right]^{n/(1-q)}, \tag{6}$$

$\alpha(x) = 3\ln x/\ln\delta_n$. Note that the singular part of the probability density function has a dependence on $\ln\delta u_n$, and that the values of $|x_n|$ are restricted within the range $[\delta_n^{\alpha_{\max}/3},\ \delta_n^{\alpha_{\min}/3}]$. The first term, $\Pi_{\rm N}^{(n)}(x_n)$ assumed to come from thermal or dissipative fluctuation caused by the kinematic viscosity, will be considered later in this paper after estimating the moments of the velocity fluctuation.

The mth moments of the velocity fluctuation, defined by $\langle\langle|x_n|^m\rangle\rangle = \int_{-\infty}^{\infty} dx_n|x_n|^m\Pi^{(n)}(x_n)$, are given by

$$\langle\langle|x_n|^m\rangle\rangle = 2\gamma_m^{(n)} + (1 - 2\gamma_0^{(n)})\ a_m\ \delta_n^{\zeta_m} \tag{7}$$

where $a_{3\bar{q}} = \{2/[C_{\bar{q}}^{1/2}(1 + C_{\bar{q}}^{1/2})]\}^{1/2}$ with $C_{\bar{q}} = 1 + 2\bar{q}^2(1-q)X\ln 2$, and

$$2\gamma_m^{(n)} = \int_{-\infty}^{\infty} dx_n\ |x_n|^m\Pi_{\rm N}^{(n)}(x_n). \tag{8}$$

Here, we used the normalization $\langle\!\langle 1 \rangle\!\rangle = 1$. The quantity

$$\zeta_m = \alpha_0 m/3 - 2Xm^2/\left[9\left(1 + C_{m/3}^{1/2}\right)\right] - \left[1 - \log_2\left(1 + C_{m/3}^{1/2}\right)\right]/(1-q), \tag{9}$$

is the so-called scaling exponents of velocity structure function, whose expression was derived first by the present authors [9–12]. In Fig. 3, we compare the present result (9) with the experimentally measured scaling exponents [16] at Re = 540 000 (circles) and Re = 69 000 (triangles). We use the observed value of the intermittency exponent, i.e., $\mu = 2 - \zeta_6 = 0.28$, for theoretical analysis. There are also represented, as references, the predictions of K41 (dotted line) [7], of She-Leveque (dashed line) [17] and of the log-normal (short-dashed line) [18–20]. Note that our formula (9) can also explain the scaling exponent for higher moments [9–12].

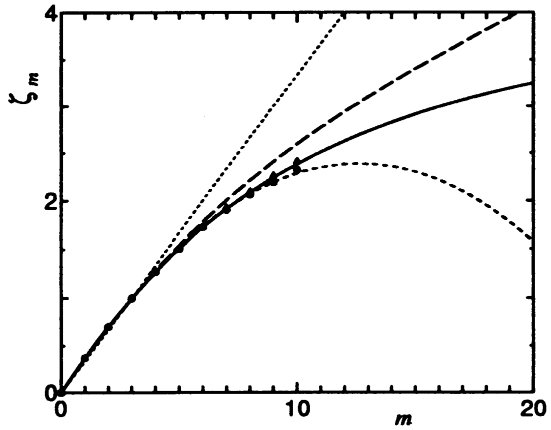

FIG. 3. The scaling exponent ζ_m of the velocity structure function. The experimental results obtained by Lewis and Swinney are shown by circles (Re = 540 000) and by triangles (Re = 69 000). The present theoretical result (9) is drawn by solid line for the intermittency exponent $\mu = 0.28$ taken from the experimental data. Dotted line represents K41, whereas dashed line She-Leveque. The prediction of the log-normal model is given by short-dashed line with the best fit but inconsistent value $\mu = 0.27$ of the intermittency exponent following Lewis and Swinney.

Let us introduce new variable

$$\xi_n = \delta u_n / \sqrt{\langle\!\langle \delta u_n^2 \rangle\!\rangle} = x_n / \sqrt{\langle\!\langle x_n^2 \rangle\!\rangle} = \bar{\xi}_n \delta_n^{\alpha/3 - \zeta_2/2} \tag{10}$$

scaled by the variance of velocity fluctuation where $\bar{\xi}_n = [2\gamma_2^{(n)} \delta_n^{-\zeta_2} + (1 - 2\gamma_0^{(n)}) a_2]^{-1/2}$, and the probability density function (PDF) $\hat{\Pi}^{(n)}(|\xi_n|)$ in terms of this variable through the relation

$$\hat{\Pi}^{(n)}(|\xi_n|)d\xi_n = \Pi^{(n)}(|x_n|)dx_n. \tag{11}$$

Making use of the relation between ξ_n and α, the PDF responsible for the distribution of singularities $\hat{\Pi}_{\mathrm{S}}^{(n)}(|\xi_n|)$ can be rewritten in terms of α in the form

$$\hat{\Pi}_{\mathrm{S}}^{(n)}(|\xi_n|) = \bar{\Pi}_{\mathrm{S}}^{(n)} \delta_n^{\zeta_2/2-\alpha/3+1-f(\alpha)} \tag{12}$$

with $\bar{\Pi}_{\mathrm{S}}^{(n)} = 3(1-2\gamma_0^{(n)})/(2\bar{\xi}_n\sqrt{2\pi X |\ln \delta_n|})$.

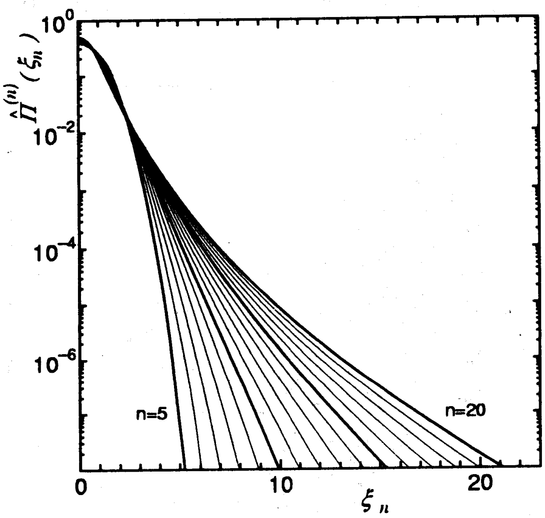

FIG. 4. The n-dependence of the PDF $\hat{\Pi}^{(n)}(\xi_n)$ given by the present analysis with $q = 0.471$ ($\mu = 0.280$) for integer values n from 5 to 20, from left to right at the axis ξ.

In the following, we will derive the symmetric part of the PDF of velocity difference. The origin of the asymmetry in the PDF (i.e., skewness) may be attributed to dissipative evolution of eddies or to experimental setup and situations. The consideration of the latter will be reported elsewhere.

In order to determine the normal part $\hat{\Pi}_{\mathrm{N}}^{(n)}(\xi_n)$ of the PDF, we divide $\hat{\Pi}^{(n)}(\xi_n)$ into two parts [21]: $\hat{\Pi}^{(n)}(\xi_n) = \hat{\Pi}_{<*}^{(n)}(\xi_n)$ for $|\xi_n| \le \xi_n^*$, and $\hat{\Pi}^{(n)}(\xi_n) = \hat{\Pi}_{*<}^{(n)}(\xi_n)$ for $\xi_n^* \le |\xi_n| \le \bar{\xi}_n \delta_n^{\alpha_{\min}/3-\zeta_2/2}$. The point ξ_n^* is defined by $\xi_n^* = \bar{\xi}_n \delta_n^{\alpha^*/3-\zeta_2/2}$ giving $\hat{\Pi}_{\mathrm{S}}^{(n)}(|\xi_n^*|) = \bar{\Pi}_{\mathrm{S}}^{(n)}$, where α^* is the solution of $\zeta_2/2 - \alpha/3 + 1 - f(\alpha) = 0$. The PDF function $\hat{\Pi}_{<*}^{(n)}(\xi_n)$ is constituted both by thermal fluctuation and by the multifractal distribution of singularities, and is assumed to be given by Gaussian function [21]. On the other hand, the contribution to $\hat{\Pi}_{*<}^{(n)}(\xi_n)$ is assumed to come only from the multifractal distribution of singularities, i.e.,

$\hat{\Pi}^{(n)}_{*<}(\xi_n) = \hat{\Pi}^{(n)}_{S}(|\xi_n|)$ [21]. Connecting $\hat{\Pi}^{(n)}_{<*}(\xi_n)$ and $\hat{\Pi}^{(n)}_{*<}(\xi_n)$ at ξ_n^* having the same value and the same derivative there, we have

$$\hat{\Pi}^{(n)}_{<*}(\xi_n) = \bar{\Pi}^{(n)}_{S} e^{-[1+3f'(\alpha^*)][(\xi_n/\xi_n^*)^2-1]/2}. \tag{13}$$

The n-dependence of $\hat{\Pi}^{(n)}(\xi_n)$ is shown in Fig. 4 with the self-consistently determined parameters α_0, X and q [21]. We notice that there are two points which look like independent of the number n of steps in the cascade at $\xi_n \approx 0.8$ and at $\xi_n \approx 2.3$. These points are also observed in the experimental data [16] at about the same values of ξ_n.

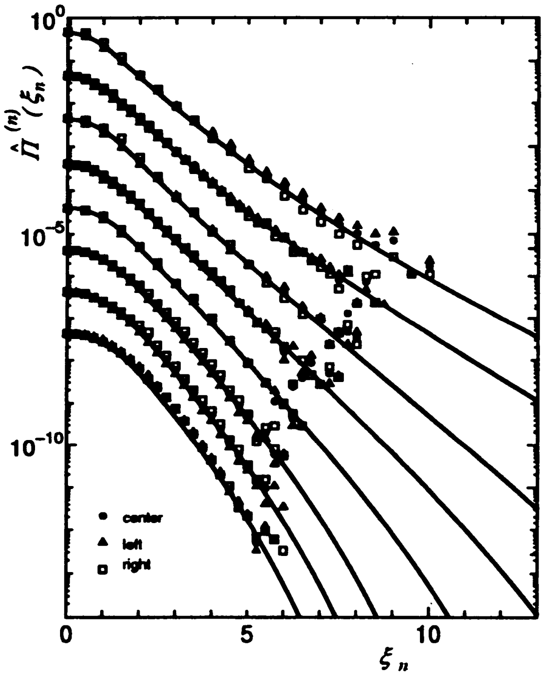

FIG. 5. Experimentally measured PDF of the velocity fluctuations by Lewis and Swinney for $R_\lambda = 262$ (Re = 540 000) are compared with the present theoretical results $\hat{\Pi}^{(n)}(\xi_n)$. Open triangles are the experimental data points on the left hand side of the PDF taken from Lewis and Swinney, whereas open squares are those on the right hand side. Closed circles are the symmetrized points obtained by taking averages of the left and the right hand experimental data. For the experimental data, the distances $r/\eta = \ell_n/\eta$ are, from top to bottom: 11.6, 23.1, 46.2, 92.5 208, 399, 830 and 1440. Solid lines represent the curves given by the present theory with $q = 0.471$. For the theoretical curves, the number of steps in the cascade n are, from top to bottom: 14, 13, 11, 10, 9.0, 8.0, 7.5, 7.0. For better visibility, each PDF is shifted by -1 unit along the vertical axis.

The comparison of experimentally measured PDF's of the velocity fluctuation [16] and those obtained by the present analysis is given in Fig. 5. In order to extract the symmetrical part from experimental data, we took mean average of those on the left hand side (represented by open triangles in the figure) and the right hand side (by open squares). The symmetrized data are described by closed circles. The solid lines are the curves

$\hat{\Pi}^{(n)}(\xi_n)$ obtained by the present analysis.

The dependence of n on r/η, extracted from Fig. 5, is shown in Fig. 6 by solid line, which gives us the best fit

$$n = -1.019 \times \log_2 r/\eta + 0.901 \times \log_2 \mathrm{Re} \tag{14}$$

with Re = 540 000. The dashed line represents (1) valid in the absence of intermittency. From (14), we see that the power w in $\mathrm{Re} = (\ell_0/\eta)^w$ turns out to be $w = 1.13$ in the present intermittent turbulence, which is 4/3 in the absence of intermittency, and that the number n_K corresponding to the Kolmogorov scale is estimated as $n_\mathrm{K} = 17.2$ for the experiments under consideration.

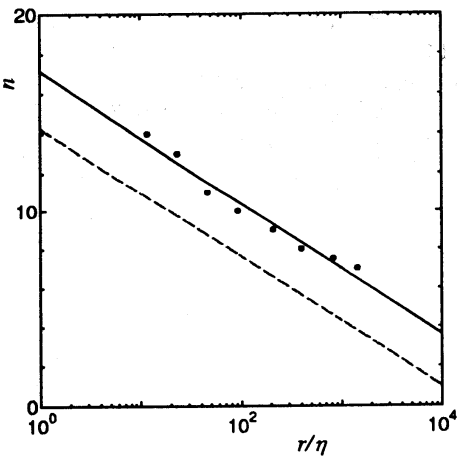

FIG. 6. Dependence of n on r/η, extracted from Fig. 5, is given by circles, which can be fitted by solid line (14). The dashed line represents (1), put for reference, which is derived in the absence of intermittency.

The success of the present theory in the analysis of the experiments [16] may indicate the robustness of singularities even for the case of no inertial range. The same experiments are investigated in [22] by a rather different analysis from the present one. Comparison of these two approaches is given in [21]. The present theory works quite well also for another systematic numerical experiments conducted by Gotoh [23]. It will be reported elsewhere.

The authors would like to thank Prof. C. Tsallis for his fruitful comments with encouragement. The authors are grateful to Prof. T. Gotoh for his kindness to show his data prior to publication.

[1] C. Tsallis, J. Stat. Phys. **52**, 479 (1988).
[2] C. Tsallis, Braz. J. Phys. **29**, 1 (1999). On the subject see also at http://tsallis.cat.cbpf.br/biblio.htm.
[3] A. Rényi, *Proc. 4th Berkley Symp. Maths. Stat. Prob.* **1**, 547 (1961).
[4] T. Arimitsu and N. Arimitsu, Phys. Rev. E **61**, 3237 (2000).
[5] C. Meneveau and K. R. Sreenivasan, Phys. Rev. Lett. **59**, 1424 (1987).
[6] C. Meneveau and K.R. Sreenivasan, Nucl. Phys. B (Proc. Suppl.) **2**, 49 (1987).
[7] A.N. Kolmogorov, C.R. Acad. Sci. USSR **30**, 301; 538 (1941).
[8] R. Benzi, G. Paladin, G. Parisi and A. Vulpiani, J. Phys. A: Math. Gen. **17**, 3521 (1984).
[9] T. Arimitsu and N. Arimitsu, J. Phys. A: Math. Gen. **33**, L235 (2000) [CORRIGENDUM: **34**, 673 (2001)].
[10] T. Arimitsu and N. Arimitsu, Chaos, Solitons and Fractals (2000) in press.
[11] T. Arimitsu and N. Arimitsu, Prog. Theor. Phys. **105**, 355 (2001).
[12] T. Arimitsu and N. Arimitsu, Physica A **295** (2001) 177.
[13] J.H. Havrda and F. Charvat, Kybernatica **3**, 30 (1967).
[14] U.M.S. Costa, M.L. Lyra, A.R. Plastino and C. Tsallis, Phys. Rev. E **56**, 245 (1997).
[15] M.L. Lyra and C. Tsallis, Phys. Rev. Lett. **80**, 53 (1998).
[16] G.S. Lewis and H.L. Swinney, Phys. Rev. E **59**, 5457 (1999).
[17] Z-S. She and E. Leveque, Phys. Rev. Lett. **72**, 336 (1994).
[18] A.M. Oboukhov, J. Fluid Mech. **13**, 77 (1962).
[19] A.N. Kolmogorov, J. Fluid Mech. **13**, 82 (1962).
[20] A.M. Yaglom, Sov. Phys. Dokl. **11**, 26 (1966).
[21] T. Arimitsu and N. Arimitsu, cond-mat/0109007 (2001).
[22] C. Beck, G.S. Lewis and H.L. Swinney, Phys. Rev. E **63**, 035303-1 (2001).
[23] T. Gotoh, D. Fukayama and T. Nakano (2001) preprint.